RARE DECAYS AT LHCb*

Fatima Soomro

on behalf of the LHCb Collaboration

CERN, Geneva 1211, Switzerland

(Received April 17, 2012)

LHCb is one of the four major experiments at the Large Hadron Collider at CERN and is custom built to look for CP violation and New Physics in rare decays of the B and D mesons. Rare decays that occur via loop diagrams provide a way to probe New Physics at energy scales much higher than can be probed by direct production. In this article, the LHCb analyses of $B \to \mu^+\mu^-$, $B_d \to K^{*0}\mu^+\mu^-$ and $B \to V\gamma$ and their results are reported.

DOI:10.5506/APhysPolB.43.1593
PACS numbers: 13.20.He, 14.40.Nd

1. Introduction

In this paper, we discuss some flavour changing neutral current (FCNC) decays of B meson. These decays are forbidden at tree level in the Standard Model (SM) and are allowed to occur only via loop diagrams. Such decays, therefore, occur rarely which makes them excellent probes of New Physics (NP), the presence of which can affect their branching fractions (BR), angular distributions and other properties. Example of such decays are: $B_{d,s} \to \mu^+\mu^-$, $B_d \to K^{*0}\mu^+\mu^-$ and $B \to V\gamma$ ($B_d \to K^*\gamma$ and $B_s \to \phi\gamma$). Inclusion of charge conjugate processes is implied through-out this article.

In this paper, we present the results obtained at LHCb with the data collected in the first half of 2011, corresponding to ~ 0.37 pb^{-1}. The excellent performance of the LHCb detector during this period has allowed high quality data to be recorded with good efficiency ($> 90\%$). The LHCb trigger allows to keep high efficiency on rare decays containing muons in the final state with dedicated single and dimuon lines in the first (hardware) and second (software) trigger levels. There are also dedicated photon lines

* Presented at the Cracow Epiphany Conference on Present and Future of B Physics, Cracow, Poland, January 9–11, 2012.

at all levels of the LHCb trigger which exploit the decay topology, *i.e.* a high-$p_{\rm T}$ photon (and two tracks), keeping high efficiency on radiative B decays. In addition, there are 'topological' triggers which are mostly relevant for hadronic B decays, but also contribute to the efficiency on rare decays, where the B decays to two muons (or a photon) and hadrons.

The details of the LHC machine and LHCb detector performance are reported by Alessio [1] in these proceedings. In the following, we discuss some rare decay analyses in detail, current results and future prospects.

2. $B^0_{(s)} \to \mu^+\mu^-$ decays at LHCb

The expression for the BR of $B^0_{(s)} \to \mu^+\mu^-$ decays can be written as [2]

$$\begin{aligned}
{\rm BR}\left(B^0_{(s)} \to \mu^+\mu^-\right) \;\propto\; & \mid V_{tb}V^*_{tq} \mid^2 \sqrt{1-\frac{4m_\mu^2}{M_{B_q}^2}} \\
& \times\left[M_{B_q}^2\left(1-\frac{4m_\mu^2}{M_{B_q}^2}\right)\left(\frac{C_{\rm S}-\frac{m_q}{m_b}C'_{\rm S}}{1+\frac{m_q}{m_b}}\right)^2\right. \\
& \left.+\left[M_{B_q}\left(\frac{C_{\rm P}-\frac{m_q}{m_b}C'_{\rm P}}{1+\frac{m_q}{m_b}}\right)+\frac{2m_\mu}{M_{B_q}}\left(C_{\rm A}-C'_{\rm A}\right)\right]^2\right],
\end{aligned}$$

where the V_{tq} are the relevant CKM factors, m_μ and M_{B_q} are the muon and B meson masses respectively, while the m_q and m_b are the quark masses. The $C_{\rm S}$, $C_{\rm P}$ and $C_{\rm A}$ denote the coefficients of scalar, pseudo-scalar and axial vector operators respectively, contributing to this decay. The primes denote the same for the helicity flipped operators.

Within the SM, $B^0_{(s)} \to \mu^+\mu^-$ is dominated by the helicity suppressed operator ($C_{\rm A}$) which is proportional to the ratio of the masses of the muon and the B hadron (m_μ/M_{B_q}). The $B^0 \to \mu^+\mu^-$ decay is further suppressed with respect to $B_s \to \mu^+\mu^-$ by the square of the ratio of CKM factors $|V_{td}|/|V_{ts}|$. The contribution of the scalar and pseudo-scalar operators ($\mathcal{C}^{(\prime)}_{\rm s,p}$) is proportional to the mass of the B hadron. In the SM, this contribution is due to Higgs exchanges and is negligible, which may not be true for NP. Hence NP can enhance the contribution of (pseudo-) scalar operators resulting in a higher BR than the SM prediction. A Feynman diagram for the $B_s \to \mu^+\mu^-$ decay in the SM and in the minimal supersymmetric standard model extention (MSSM) is shown in Fig. 1, left and right, respectively.

The SM predicts ${\rm BR}(B_s \to \mu^+\mu^-) = (3.2 \pm 0.2) \times 10^{-9}$ [3] while the best upper limit from experiment is set by LHCb to be ${\rm BR}(B_s \to \mu^+\mu^-) < 1.6 \times 10^{-8}$ [4]. A combination of this result with the CMS experiment gives

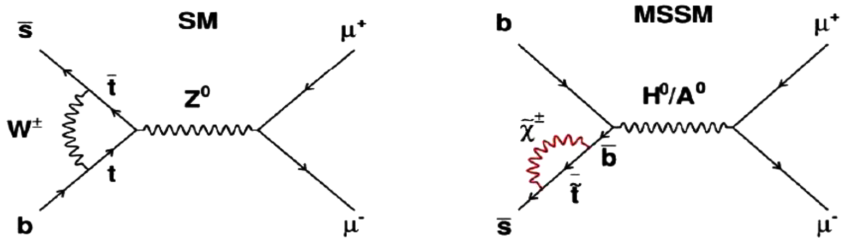

Fig. 1. Left: $B_s \to \mu^+\mu^-$ diagram in the SM. Right: A possible $B_s \to \mu^+\mu^-$ diagram in the MSSM model.

an upper limit of 1.1×10^{-8} [5]. Although this limit is about 3 times the SM prediction, it puts strong constraints on some NP scenarios. A detailed study of the impact of the $B \to \mu^+\mu^-$ limits on the different SUSY scenarios is reported in reference [6].

2.1. Analysis strategy

The $B^0_{(s)} \to \mu^+\mu^-$ search is performed in a two dimensional plane of the dimuon invariant mass ($m_{\mu^+\mu^-}$) and a multivariate variable (BDT) which is the output of a Boosted Decision Tree (using the TMVA package). The plane is divided into 24 bins, 6 in mass and 4 in BDT. In each bin of this plane, the expected number of signal and background is estimated and then the compatibility of the observed number of events with background-only and background plus signal hypotheses is computed. This information from each bin is used to compute the final limit using the $\mathrm{CL_s}$ method [7]. In order to avoid any potential bias, the events in the signal region, defined as $M_{B^0} - 60$ MeV to $m_{B_s} + 60$ MeV, were blinded until all the analysis choices were finalized.

The variables used in the building of the BDT are the proper time, impact parameter (IP), p_{T} and isolation of the B candidate, the distance of closest approach of the two muons, minimum of the p_{T} of the two muons, sum of the isolation of the muons, minimum of the IP of the two muons and the muon polar angle [4, 8]. The BDT is trained on $b\bar{b} \to \mu^+\mu^- X$ and $B_s \to \mu^+\mu^-$ Monte Carlo (MC) samples and then calibrated in data. To calibrate the shape of the signal and combinatorial background in the BDT axis, we use $B^0_{(s)} \to h^+h'^-$ decays (where $h^{(\prime)} = K$ or π) and $B^0_{(s)} \to \mu^+\mu^-$ candidates from the mass sidebands, respectively. The distribution of signal and background in BDT as obtained from data using the above procedure is shown in Fig. 2. The invariant mass line shape of the signal events is parametrized with a Crystal Ball function. The mean values of the mass of the B^0 and B_s mesons are obtained from the $B^0 \to K\pi$ and $B_s \to KK$

decays in data. The resolutions are extracted from data with a linear interpolation between the measured resolutions of charmonium and bottomonium resonances decaying into two muons. The combinatorial background shape in mass is parametrized as an exponential, the exponent of which is computed using the mass sidebands, separately in each BDT bin.

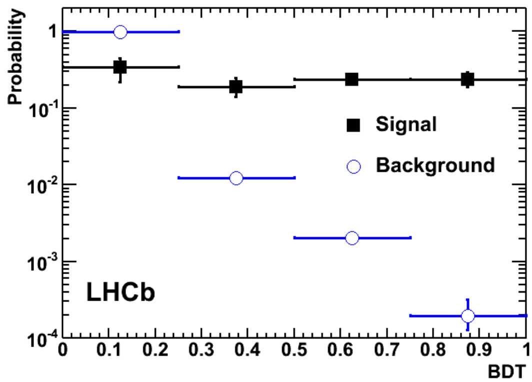

Fig. 2. Distribution of signal (solid square) and background (open circles) in BDT obtained from $B^0_{(s)} \to h^+h'^-$ signal and $B^0_{(s)} \to \mu^+\mu^-$ mass sidebands in data.

The level of the peaking background due to doubly misidentified $B^0_{(s)} \to h^+h'^-$ events is evaluated by measuring the $\epsilon(K \to \mu)$ and $\epsilon(\pi \to \mu)$ misidentification rates in data (with $D^0 \to K\pi$ channel) and normalizing it with the $B^0_{(s)} \to h^+h'^-$ yield in data. The shape of this background component in BDT and mass is obtained using an MC sample which is a mixture of the various $B^0_{(s)} \to h^+h'^-$ decays in a proportion that takes into account their BR and the relevant hadronization fraction $f_{s,d}$. The distribution of the $B^0_{(s)} \to \mu^+\mu^-$ candidates in the dimuon invariant mass and BDT plane, observed in the 0.37 fb^{-1} dataset is shown in Fig. 3.

To extract the level, the $B^0_{(s)} \to \mu^+\mu^-$ signal is normalized to other well known B decays so as to avoid relying on the calculation of absolute efficiencies and luminosity

$$\mathrm{BR} = \mathrm{BR}_{\mathrm{cal}} \times \frac{\epsilon^{\mathrm{REC}}_{\mathrm{cal}} \epsilon^{\mathrm{SEL|REC}}_{\mathrm{cal}}}{\epsilon^{\mathrm{REC}}_{\mathrm{sig}} \epsilon^{\mathrm{SEL|REC}}_{\mathrm{sig}}} \frac{\epsilon^{\mathrm{TRIG|SEL}}_{\mathrm{cal}}}{\epsilon^{\mathrm{TRIG|SEL}}_{\mathrm{sig}}} \times \frac{f_{\mathrm{cal}}}{f_{B_s}} \times \frac{N_{B^0_{(s)} \to \mu^+\mu^-}}{N_{\mathrm{cal}}} \,,$$

where the subscript denotes the signal or normalization channel.

The reconstruction and selection efficiencies are taken from MC and cross checked with data, the trigger efficiency is obtained from data using J/ψ and reweighted for the signal spectrum from MC, and the LHCb measurement of $\frac{f_s}{f_d} = 0.267^{+0.021}_{-0.020}$ [9] is used.

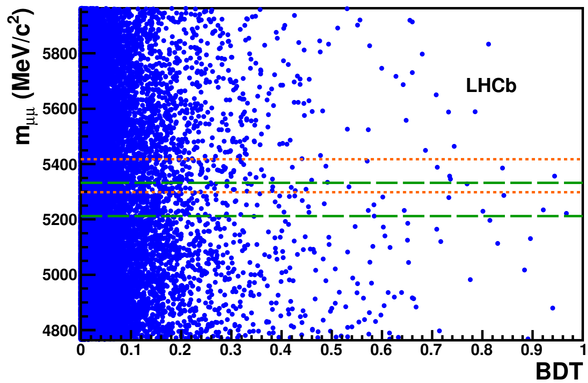

Fig. 3. Observed distribution of events in the $m_{\mu^+\mu^-}$ and BDT plane, for 0.37 fb^{-1} of LHCb data. The horizontal lines represent the blinded B_d and B_s mass windows.

We use three normalization channels, namely $B_s \to J/\psi\,\phi$, $B^+ \to J/\psi\,K^+$ and $B^0 \to K^+\pi^-$, which have a different number of final state particles and involve different systematics. The final normalization is taken as a weighted average of the normalization factors.

2.2. Results and prospects

The analysis with 0.37 fb^{-1} of the 2011 LHCb data results in the upper limits of [4]:

- $\mathrm{BR}(B_s \to \mu^+\mu^-) < 1.6 \times 10^{-8}$,
- $\mathrm{BR}(B^0 \to \mu^+\mu^-) < 3.6 \times 10^{-9}$

at 95% confidence limit. The $\mathrm{CL_s}$ distribution for $B_s \to \mu^+\mu^-$ is shown in Fig. 4.

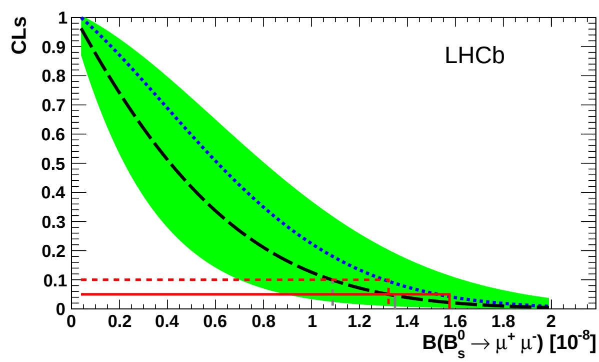

Fig. 4. The $B_s \to \mu^+\mu^-$ $\mathrm{CL_s}$ distribution, using 0.37 fb^{-1} of the 2011 data.

If the current analysis is projected to an integrated luminosity of 1 fb^{-1}, the median of the 95% confidence level is around $\mathrm{BR}(B_s \to \mu^+\mu^-) = 8 \times 10^{-9}$. Fig. 5 shows the potential of a 3σ discovery, projecting the sensitivity of the current analysis. Therefore, there is a chance to discover $B_s \to \mu^+\mu^-$ with the full 2011 data set if the SM prediction of its BR holds.

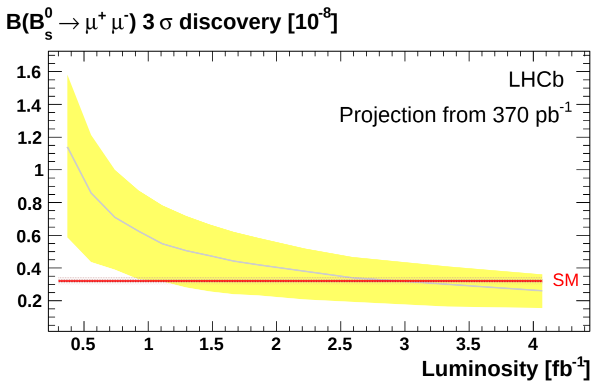

Fig. 5. From the current analysis, projection of a 3σ discovery for different BRs as a function of integrated luminosity.

3. $b \to s\ell^+\ell^-$ and $b \to s\gamma$ decays

B decays to a meson and a photon or lepton pair are dominated by the operators O_7 and $O_{9,10}$ in the SM. These decays have a rich phenomenology and are sensitive to many NP attributes. For example, the differential BR of $B_d \to K^{*0}\mu^+\mu^-$ is sensitive to the mass scale and couplings of NP operators. The angular distribution of this decay is sensitive to the helicity structure of NP operators, so is the CP asymmetry in the $B_s \to \phi\gamma$ decay. Table I summarises the NP reach sensitivity of many decays that occur via the quark level $b \to s$ transition.

In the following, we describe the A_{FB} measurement in $B_d \to K^{*0}\mu^+\mu^-$ and the measurement of $\mathrm{BR}(B_s \to \phi\gamma)$.

3.1. A_{FB} in $B_d \to K^{*0}\mu^+\mu^-$

The forward–backward asymmetry or A_{FB} in $B_d \to K^{*0}\mu^+\mu^-$ is defined as the difference between the number of positive and negative leptons going in the same direction as the s quark, in the dilepton rest frame. At LHCb, the analysis is performed in 6 bins of q^2 (invariant mass of the muon pair).

The parameters A_{FB} and F_{L}, the longitudinal polarization of the K^{*0} are extracted by performing a simultaneous fit to the mass θ_l and θ_K in bins if q^2, explicitly:

TABLE I

Summary of the NP properties that can be probed with various $b \to s\ell^+\ell^-$ and $b \to s\gamma$ decays.

Measurement	Decay mode	NP properties
Differential BR and angular distributions	$B_d \to K^{*0}\mu^+\mu^-$ $B^+ \to K^+\mu^+\mu^-$ $\Lambda_b \to \Lambda^{(*)}\mu^+\mu^-$ $B_s \to \phi\mu^+\mu^-$	Mass scale, couplings and helicity structure of NP operators
Isospin and CP asymmetries	$B_d \to K^{*0}\mu^+\mu^-$ $B^+ \to K^+\mu^+\mu^-$	Very small in SM, can be enhanced due to NP
Time dependent CP asymmetry	$B_s \to \phi\gamma$	Helicity structure of NP

$$\frac{1}{\Gamma}\frac{d^2\Gamma}{d\cos\theta_l dq^2} = \tfrac{3}{4}F_{\rm L}\left(1-\cos^2\theta_l\right) + \tfrac{3}{8}\left(1-F_{\rm L}\right)\left(1+\cos^2\theta_l\right) + A_{\rm FB}\cos\theta_l\,,$$
$$\frac{1}{\Gamma}\frac{d^2\Gamma}{d\cos\theta_K dq^2} = \tfrac{3}{2}F_{\rm L}\cos^2\theta_K + \tfrac{3}{4}\left(1-F_{\rm L}\right)\left(1-\cos^2\theta_K\right)\,.$$

The angle θ_K is the angle between the direction of the kaon in the K^{*0} rest frame and the K^{*0} in the B_d meson rest frame, while θ_l is the angle between the direction of the $\mu^+(\mu^-)$ in the dimuon rest frame and the dimuon direction in the B_d $(\bar{B}_d)$ meson rest frame as shown in Fig. 6.

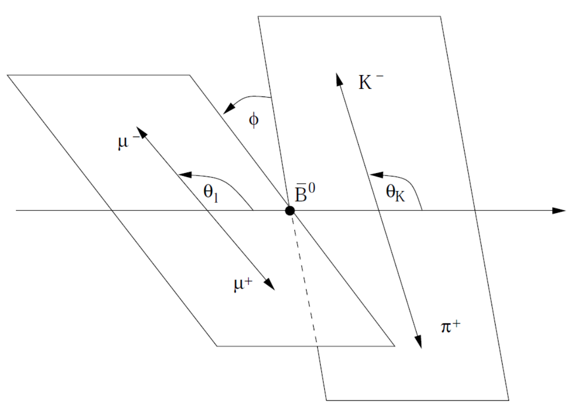

Fig. 6. Definition of the angles used in the $B_d \to K^{*0}\mu^+\mu^-$ analysis to extract $A_{\rm FB}$ and $F_{\rm L}$ [10].

The combinatorial background is rejected by cutting on the output of a Boosted Decision Tree which is trained on $B_d \to J/\psi\, K^{*0}$ signal in data and background candidates from the upper mass sidebands in the 2010 dataset.

Peaking backgrounds due to misidentification of the final state particles are reduced to a level of $< 3\%$ of the signal by using the particle identification (PID) information from the LHCb RICH (Ring Imaging Cherenkov) detectors. In particular, the probability to swap the B_d flavour, *i.e.* $B_d \leftrightarrow \bar{B}_d$, is reduced to $< 0.7\%$.

The signal events in the 0.37 fb^{-1} data, in each q^2 bin are shown in Fig. 7. The total yield from this sample is about 300 $B_d \to K^{*0}\mu^+\mu^-$ events, with a significance of 5σ or greater in each of the six q^2 bins [11].

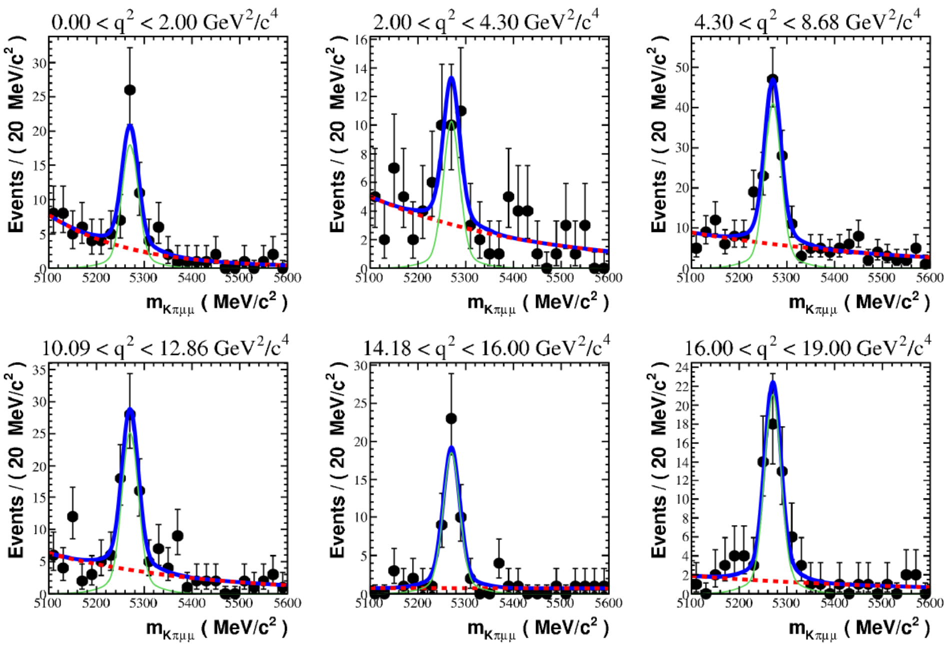

Fig. 7. The $B_d \to K^{*0}\mu^+\mu^-$ signal in each q^2 bin used in the analysis. The plots correspond to a luminosity of 0.37 fb^{-1} [11].

Since the analysis involves fitting angular variables, the detector and selection effects on the angular acceptance need to be taken into account. The acceptance effects are corrected on per event basis, by assigning weights to events, where the weights are obtained from MC which has been corrected for known discrepancies with data. This method for correcting the angular acceptance is validated on the control channel $B_d \to J/\psi\, K^{*0}$ which has a known angular distribution [11].

Figs. 8 to 10 show the LHCb results for the $A_{\rm FB}$, differential BR and $F_{\rm L}$ respectively, with 0.37 fb^{-1} [11]. The LHCb results are the most precise to date, and are compatible with the SM theoretical predictions [12] which are also plotted in the figures.

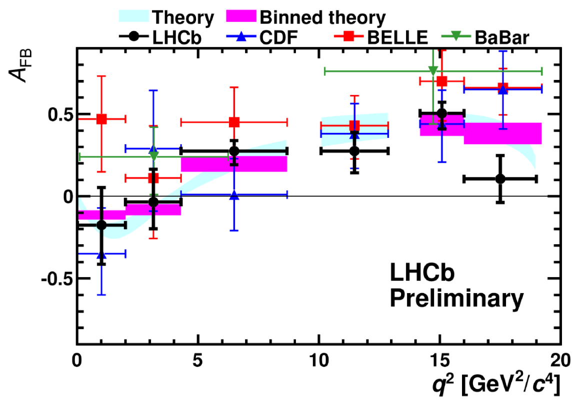

Fig. 8. The LHCb result for the $A_{\rm FB}$ in $B_d \to K^{*0}\mu^+\mu^-$ (black points, 0.37 fb^{-1}) compared to other measurements [13] and theoretical predictions from [12].

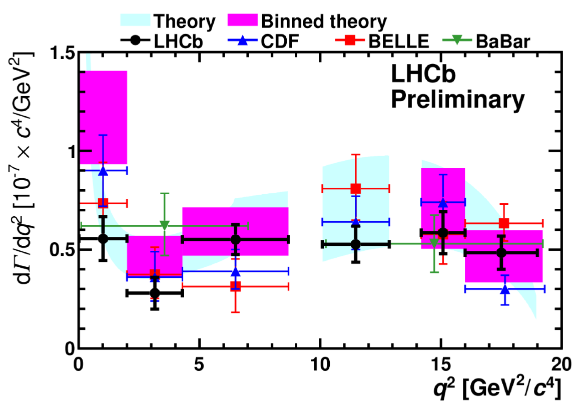

Fig. 9. The LHCb result for the differential BR of $B_d \to K^{*0}\mu^+\mu^-$ (black points, 0.37 fb^{-1}) compared to other measurements [13] and theoretical predictions from [12].

The analysis is being updated with the full 1 fb^{-1} data sample which will allow even more precision on these observables and the measurement of others, like $S3$ and $A_{(Im)}$, which are also sensitive to NP [10].

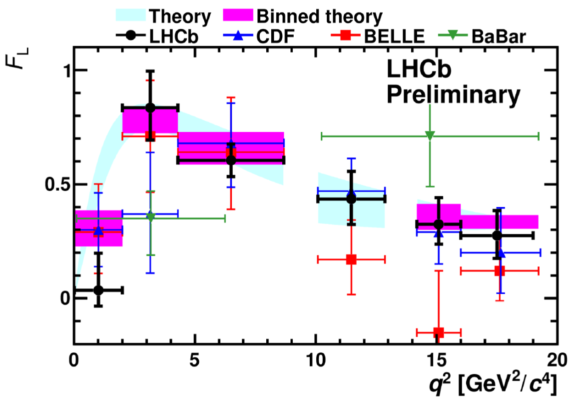

Fig. 10. The LHCb result for the longitudinal polarization F_{L} of the K^{*0} in $B_d \to K^{*0}\mu^+\mu^-$ (black points, 0.37 fb^{-1}) compared to other measurements [13] and theoretical predictions from [12].

3.2. $B_d \to K^*\gamma$ and $B_s \to \phi\gamma$

The $B_s \to \phi\gamma$ is one of the key channels at LHCb, and the aim is to measure the photon polarization in this decay, since it is sensitive to the structure of NP operators [14]. This is because in the quark level decay $b \to s\gamma$, the emitted photon is predominantly left-handed and the amplitude for the emission of a right-handed photon (F_{R}) being suppressed by the ratio of quark masses

$$\frac{F_{\mathrm{R}}}{F_{\mathrm{L}}} \approx \frac{m_s}{m_b}\,.$$

The ratio of "wrong" helicity photons in a $\bar{B}$ (or B) decay is predicted in the SM to be $\sim 0.4\%$. This ratio can be enhanced up to 10% in NP models with a helicity structure different from the SM [15]. This enhancement is possible even without affecting the rate of $b \to s\gamma$ transitions. This is important since the inclusive branching fraction $B(B \to X_s\gamma)$ has been measured to be $(3.56 \pm 0.26) \times 10^{-4}$ [16] which is compatible with the SM prediction of $(3.15 \pm 0.23) \times 10^{-4}$ [17].

The photon polarization can be measured indirectly in the time dependent decay rates of the decays of type $B \to V_{\mathrm{CP}}\gamma$, *i.e.*, where the vector meson decays into a CP eigenstate. The B factories have performed this measurement using $B_d \to K^{*0}(K_s^0\pi^0)\gamma$ decays [18]. The relevant parameter is

$$\sin 2\psi = 0.28 \pm 0.44\,.$$

At LHCb, this analysis will require ≥ 2 fb^{-1} of integrated luminosity, however, with a 0.34 fb^{-1} sample, LHCb has made the most precise measurement of $B_s \to \phi\gamma$ by measuring the ratio of $\mathrm{BR}(B_d \to K^*\gamma)/\mathrm{BR}(B_s \to \phi\gamma)$. This ratio can be written as

$$\frac{\mathrm{BR}(B_d \to K^*\gamma)}{\mathrm{BR}(B_s \to \phi\gamma)} = \frac{N_{B_d\to K^*\gamma}}{N_{B_s\to\phi\gamma}} \frac{\mathrm{BR}(\phi \to KK)}{\mathrm{BR}(K^{*0} \to K\pi)} \frac{f_s}{f_d} \frac{\epsilon_{B_s\to\phi\gamma}}{\epsilon_{B_d\to K^*\gamma}},$$

where the ratio of efficiencies can be factorized to

$$\frac{\epsilon_{B_s\to\phi\gamma}}{\epsilon_{B_d\to K^*\gamma}} = r_{\mathrm{acc}} \times r_{\mathrm{reco\ \&\ sel}} \times r_{\mathrm{PID}} \times r_{\mathrm{trigger}}\,.$$

The offline selections for $B_d \to K^*\gamma$ and $B_s \to \phi\gamma$ are the same except for the mass windows for the K^{*0} and ϕ and PID requirements on their daughters. The acceptance, selection and trigger efficiency ratios are evaluated in MC and the PID efficiency ratio is determined in data.

The large sample of $B_d \to K^*\gamma$ decay has also allowed for the calibration of the LHCb calorimeter in the high energy regime of > 2 GeV, Fig. 11 shows the result of the calibration, after which the width of the $B_d \to K^*\gamma$ signal is equal to the one predicted by the MC.

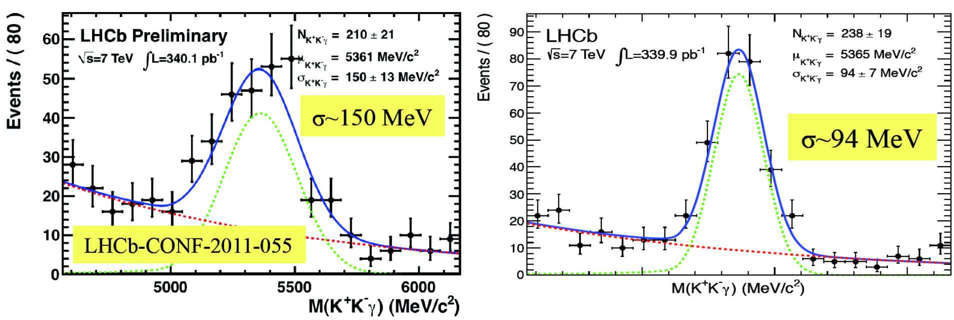

Fig. 11. The $B_d \to K^*\gamma$ mass peak before (top) and after (bottom) calorimeter calibration. The plots correspond to 0.34 fb^{-1}.

The ratio of branching fractions is measured to be [19]

$$\frac{\mathrm{BR}(B_d \to K^*\gamma)}{\mathrm{BR}(B_s \to \phi\gamma)} = 1.52 \pm 0.14\,(\mathrm{stat}) \pm 0.10\,(\mathrm{syst}) \pm 0.12(f_s/f_d)\,.$$

This result can be compared to the SM prediction of $(1.0 \pm 0.2) \times 10^{-4}$. Assuming the central value of $\mathrm{BR}(B_d \to K^*\gamma)$ from PDG, this ratio can be translated into a measurement of

$$\mathrm{BR}(B_s \to \phi\gamma) = (2.8 \pm 0.5) \times 10^{-4}$$

which improves the precision on this branching fraction by a factor of 3.

4. Conclusions

We presented a few rare decays analyses from LHCb based on about one third (0.37 fb^{-1}) of the data collected in 2011. The search for $B_s \to \mu^+\mu^-$ decays has produced the most strict upper limits on the BR of this decay and has ruled out a lot of phase space of some SUSY scenarios [6]. Further improvement in the upper limit along with the possibility of the discovery of $B_s \to \mu^+\mu^-$ is foreseen with the analysis of the entire data set collected in 2011 (1 fb^{-1}).

LHCb has also produced the most precise measurements of the $A_{\rm FB}$, $F_{\rm L}$ and differential BR measurements in $B_d \to K^{*0}\mu^+\mu^-$ decays. More variables, also sensitive to NP, will be measured with the analysis of the full 2011 dataset.

Also reported was the most precise measurement of the BR$(B_s \to \phi\gamma)$ made by LHCb, which is a factor of 3 better than the current precision. This analysis paves the way for more complicated and high statistics measurements like the direct CP asymmetry in $B_d \to K^*\gamma$ and photon polarization in $B_s \to \phi\gamma$.

These measurements are part of the diverse and expanding rare decays program of LHCb, which is already competitive with direct searches in terms of constraining NP phase space. This program will become very important in distinguishing different models once NP is discovered, hopefully soon, at the LHC.

REFERENCES

[1] F. Alessio, *Acta Phys. Pol. B* **43**, 1399 (2012), this issue.
[2] C. Bobeth, T. Ewerth, F. Kruger, J. Urban, *Phys. Rev.* **D64**, 074014 (2001).
[3] A.J. Buras, M.V. Carlucci, S. Gori, G. Isidori, *J. High Energy Phys.* **1010**, 009 (2010).
[4] LHCb Collaboration, *Phys. Lett.* **B708**, 55 (2012).
[5] LHCb Collaboration, Search for the Rare Decay $B_s \to \mu^+\mu^-$ at the LHC with the CMS and LHCb Experiments, LHCb-CONF-2011-047, 2011.
[6] A.G. Akeroyd, F. Mahmoudi, D. Martinez Santos, *J. High Energy Phys.* **12**, 88 (2011).
[7] A.L. Read, *J. Phys. G: Nucl. Part. Phys.* **28**, 2693 (2002).
[8] LHCb Collaboration, *Phys. Lett.* **B699**, 330 (2011).
[9] LHCb Collaboration, *Phys. Rev. Lett.* **107**, 211801 (2011).
[10] U. Egede *et al.*, *J. High Energy Phys.* **11**, 032 (2008).
[11] LHCb Collaboration, *Phys. Rev. Lett.* **108**, 181806 (2012) [`arXiv:1112.3515 [hep-ex]`].
[12] C. Bobeth, G. Hiller, D. van Dyk, *J. High Energy Phys.* **07**, 067 (2011).

[13] BaBar Collaboration, *Phys. Rev.* **D79**, 031102 (2009); Belle Collaboration, *Phys. Rev. Lett.* **103**, 171801 (2009); CDF Collaboration, *Phys. Rev. Lett.* **106**, 161801 (2011).

[14] D. Atwood, M. Gronau, A. Soni, *Phys. Rev. Lett.* **79**, 185 (1997).

[15] T. Goto *et al.*, *Phys. Rev.* **D70**, 035012 (2004).

[16] Belle Collaboration, *Phys. Rev. Lett.* **103**, 241801 (2009).

[17] M. Misiak *et al.*, *Phys. Rev. Lett.* **98**, 022002 (2007).

[18] Heavy Flavour Averaging Group, `arXiv:0808.1297 [hep-ex]`.

[19] LHCb Collaboration, Measurement of the Ratio of Branching Fractions $\mathcal{B}(B_d \to K^*\gamma)/\mathcal{B}(B_s \to \phi\gamma)$ with the LHCb Experiment at $\sqrt{s} = 7\,\mathrm{TeV}$, LHCb-CONF-2011-055, 2011.